

Electronic Supplementary Information for

**Chiral resolution a racemic macrocyclic complex by
recognition one enantiomer over the other: structures and
DFT calculations**

Guang-Chuan Ou, Zi-Zhou Wang, Li-Zi Yang, Cun-Yuan Zhao, and Tong-Bu Lu*

Table S1. Selected Bond Distances (Å) and Angles(°)

Δ -1			
Ni(1)-N(4)	2.084(4)	Ni(1)-N(1)	2.129(4)
Ni(1)-N(3)	2.117(5)	Ni(1)-N(2)	2.089(4)
Ni(1)-O(2)	2.139(3)	Ni(1)-O(1)	2.199(3)
N(4)-Ni(1)-N(3)	85.40(16)	N(4)-Ni(1)-O(1)	102.03(14)
O(2)-Ni(1)-O(1)	60.97(12)	N(2)-Ni(1)-N(3)	92.06(16)
N(2)-Ni(1)-O(1)	154.10(14)	N(1)-Ni(1)-O(2)	85.54(15)
N(2)-Ni(1)-N(1)	85.52(16)	N(3)-Ni(1)-N(1)	175.16(16)
N(4)-Ni(1)-N(1)	91.10(16)	N(2)-Ni(1)-O(2)	93.48(14)
N(4)-Ni(1)-O(2)	162.10(14)	N(3)-Ni(1)-O(1)	88.17(14)
N(1)-Ni(1)-O(1)	95.83(15)	N(4)-Ni(1)-N(2)	103.80(15)
N(3)-Ni(1)-O(2)	98.81(14)		
N(5)...O(4)#1	2.999(7)	N(5)-H(5C)...O(4)#1	151.8
N(5)...O(5)#1	3.084(7)	N(5)-H(5C)...O(5)#1	137.5
N(5)...O(3)#2	2.876(6)	N(5)-H(5D)...O(3)#2	135.0

A-1

Ni(1)-N(4)	2.079(4)	Ni(1)-N(2)	2.087(4)
Ni(1)-N(3)	2.123(4)	Ni(1)-O(2)	2.132(3)
Ni(1)-N(1)	2.132(4)	Ni(1)-O(1)	2.189(3)
N(4)-Ni(1)-N(2)	103.98(15)	N(3)-Ni(1)-O(2)	98.76(14)
O(2)-Ni(1)-N(1)	85.80(14)	N(4)-Ni(1)-N(3)	85.66(16)
N(4)-Ni(1)-N(1)	90.67(16)	N(4)-Ni(1)-O(1)	101.76(14)
N(2)-Ni(1)-N(3)	91.96(16)	N(2)-Ni(1)-N(1)	85.49(16)
N(2)-Ni(1)-O(1)	154.22(14)	N(4)-Ni(1)-O(2)	162.05(14)
N(3)-Ni(1)-N(1)	174.91(15)	N(3)-Ni(1)-O(1)	88.35(14)
N(2)-Ni(1)-O(2)	93.30(14)	N(1)-Ni(1)-O(1)	95.87(15)
O(2)-Ni(1)-O(1)	61.24(12)		
N(5)...O(4)#3	2.989(6)	N(5)-H(5C)...O(4)#3	141.4
N(5)...O(5)#3	3.054(6)	N(5)-H(5D)...O(5)#3	149.2
N(5)...O(3)#4	2.872(6)	N(5)-H(5D)...O(3)#4	145.6

S-2

Ni(1)-N(1)	1.931(3)	Ni(1)-N(2)	1.930(4)
Ni(1)-N(3)	1.943(3)	Ni(1)-N(4)	1.917(4)
N(4)-Ni(1)-N(2)	178.95(17)	N(4)-Ni(1)-N(1)	92.89(16)
N(2)-Ni(1)-N(1)	87.19(17)	N(2)-Ni(1)-N(3)	92.32(16)
N(4)-Ni(1)-N(3)	87.53(16)	N(1)-Ni(1)-N(3)	175.85(18)

R-2

Ni(1)-N(1)	1.941(2)	Ni(1)-N(2)	1.922(3)
Ni(1)-N(3)	1.936(3)	Ni(1)-N(4)	1.937(3)
N(2)-Ni(1)-N(3)	92.94(13)	N(2)-Ni(1)-N(4)	179.17(13)

N(3)-Ni(1)-N(4)	87.12(13)	N(3)-Ni(1)-N(1)	175.47(15)
N(2)-Ni(1)-N(1)	87.74(13)	N(4)-Ni(1)-N(1)	92.13(13)

Δ-3

Ni(1)-N(4)	2.079(5)	Ni(1)-N(2)	2.086(5)
Ni(1)-N(3)	2.121(6)	Ni(1)-O(1)	2.139(4)
Ni(1)-N(1)	2.121(6)	Ni(1)-O(2)	2.178(4)
N(4)-Ni(1)-N(2)	103.27(19)	N(4)-Ni(1)-N(3)	85.6(2)
N(2)-Ni(1)-N(3)	91.2(2)	N(1)-Ni(1)-O(1)	86.7(2)
N(4)-Ni(1)-N(1)	91.6(2)	N(4)-Ni(1)-O(2)	94.33(18)
N(2)-Ni(1)-N(1)	85.0(2)	N(2)-Ni(1)-O(2)	161.92(18)
N(3)-Ni(1)-N(1)	174.67(18)	N(3)-Ni(1)-O(2)	86.02(19)
N(4)-Ni(1)-O(1)	154.86(17)	N(1)-Ni(1)-O(2)	98.74(18)
N(2)-Ni(1)-O(1)	101.56(18)	O(1)-Ni(1)-O(2)	61.27(15)
N(3)-Ni(1)-O(1)	97.7(2)		
N(5)...O(10)#5	2.964(8)	N(5)-H(5C)...O(10)#5	110.6
N(5)...O(8)#6	2.929(8)	N(5)-H(5B)...O(8)#6	157.0

Λ-3

Ni(1)-N(4)	2.079(3)	Ni(1)-N(2)	2.084(3)
Ni(1)-N(1)	2.116(4)	Ni(1)-O(1)	2.138(3)
Ni(1)-N(3)	2.129(3)	Ni(1)-O(2)	2.183(3)
N(4)-Ni(1)-N(2)	103.66(12)	N(4)-Ni(1)-N(1)	91.31(13)
N(2)-Ni(1)-N(1)	85.64(13)	N(4)-Ni(1)-O(1)	101.34(11)
N(4)-Ni(1)-N(3)	85.18(13)	N(2)-Ni(1)-O(1)	154.67(11)
N(2)-Ni(1)-N(3)	91.69(13)	N(1)-Ni(1)-O(1)	97.87(12)
N(1)-Ni(1)-N(3)	174.97(12)	N(3)-Ni(1)-O(1)	86.37(12)

N(1)-Ni(1)-O(2)	86.18(12)	N(4)-Ni(1)-O(2)	161.69(11)
N(3)-Ni(1)-O(2)	98.27(11)	N(2)-Ni(1)-O(2)	94.24(11)
O(1)-Ni(1)-O(2)	61.18(10)		
N(5)...O(10)#7	2.966(5)	N(5)-H(5A)...O(10)#7	115.0
N(5)...O(8)#8	2.927(5)	N(5)-H(5B)...O(8)#8	163.9

^aSymmetry transformations used to generate equivalent atoms: #1 $-x+1, y+1/2, -z+1$, #2 $-x+2, -y+1, z-1/2$, #3 $y+1, -x+1, z-3/4$, #4 $-x+2, -y+1, z-1/2$, #5 $-x+2, -y+1, z-1/2$, #6 $y+1, -x+1, z-1/4$, #7 $-y+1, x-1, z-1/4$, #8 $x, y-1, z$.

Table S2 The single-point energy (E) for the cations of $\Delta-1$, $\Lambda-1$, $\Delta-3$ and $\Lambda-3$ at the B3LYP/6-31G(d) (LANL2DZ for Ni) Level.

Compound	E
$\Delta-1$	-1460.4539100
$\Delta-3$	-1460.2308702
$\Lambda-3$	-1460.2342387
$\Lambda-1$	-1460.4559491

Table S3 The numbers of Imaginary Frequencies for the cations of $\Delta-1$, $\Lambda-1$, $\Delta-3$ and $\Lambda-3$ at the B3LYP/6-31G(d) (LANL2DZ for Ni) Level.

$\Delta-1$	$\Lambda-1$	$\Delta-3$	$\Lambda-3$
-1448.4677	-1450.9619	-1442.2215	-1443.9389
-1196.3239	-1187.5217	-1188.8201	-1193.6001
-1184.4595	-1184.5047	-1186.0610	-1187.0691
-1184.1220	-1181.9245	-1183.8579	-1185.3765
-1182.8624	-1178.6411	-1182.8670	-1180.8355
-1182.2799	-1177.2634	-1181.9493	-1179.6744
-1175.6539	-1175.0878	-1178.8327	-1177.7408
-1172.2074	-1168.7899	-1169.3865	-1170.2324
-1165.9303	-1166.5274	-1165.4854	-1164.1401
-1014.5113	-1021.9366	-1003.3935	-1004.7568

-980.9521	-980.9800	-970.8139	-975.3660
-878.1556	-878.4490	-879.2624	-881.2403
-872.3779	-875.4731	-878.4842	-875.3714
-863.1574	-857.9260	-863.8263	-867.0978
-819.6217	-822.5477	-815.3462	-818.6395
-813.6699	-807.1066	-811.5078	-817.9127
-787.2633	-791.3833	-784.6059	-785.7564
-777.1907	-774.6575	-781.2427	-784.3072
-776.7544	-772.3204	-774.7506	-778.3078
-761.5519	-767.1134	-765.7821	-765.0227
-751.1905	-747.7872	-750.7037	-751.9326
-748.8146	-745.8689	-743.5534	-749.1311
-745.0504	-742.8261	-740.8626	-746.1030
-739.6226	-739.6498	-740.1689	-740.1865
-733.6696	-722.9597	-724.6913	-733.9056
-714.3516	-710.7086	-715.2687	-719.0956
-708.8633	-708.5826	-709.4886	-706.8816
-699.7736	-702.9160	-705.9640	-706.0301
-698.9721	-697.5368	-702.5416	-701.5693
-695.0998	-693.6167	-699.2493	-700.8771
-690.6669	-687.5521	-696.2250	-695.4074
-685.4134	-684.1551	-686.8411	-689.8472
-676.0028	-679.2208	-682.9521	-688.1700
-673.0806	-663.8153	-677.0394	-676.5387
-661.2705	-655.8019	-663.1357	-667.9410
-652.0875	-636.3043	-660.3857	-657.4119
-592.2269	-609.6638	-587.6265	-601.4694
-553.7395	-579.6866	-566.7139	-581.3100
-248.3203	-250.4284	-240.5629	-239.3608
-239.4148	-232.5338	-235.2356	-234.7197
-213.1084	-208.7392	-208.2215	-210.7294
-150.8574	-150.8297	-152.8979	-156.5626
-145.7531	-146.1377	-136.7645	-136.8127
-116.7686	-114.9218	-129.6216	-130.1036
-101.0331	-96.0636	-102.5970	-109.3709
-79.2700	-74.9762	-57.2858	-60.5927
	-36.5706	-46.0224	-55.6442

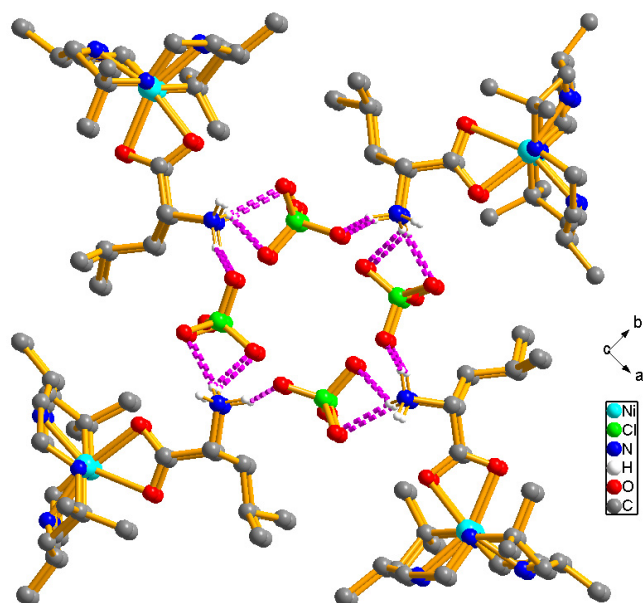


Figure S1. 1D hydrogen bonded right-handed helical chains in Δ -1 along the 4_1 axis.

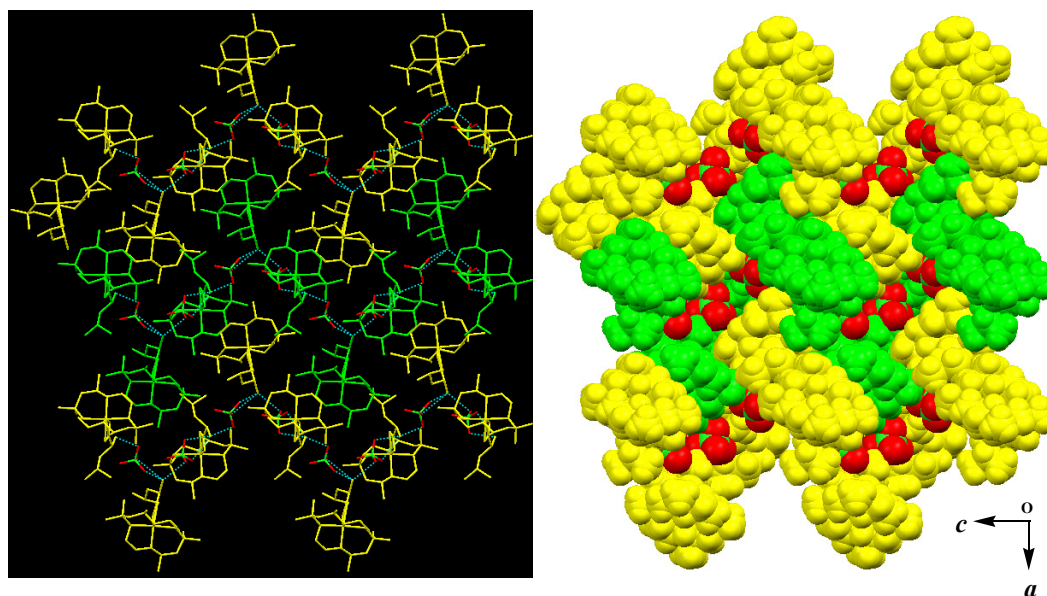


Figure S2. The congregations of right-handed helical chains (marked as yellow and green colour) through the zipper-like interchain hydrophobic interactions in Δ -1 along the 4_1 axis.

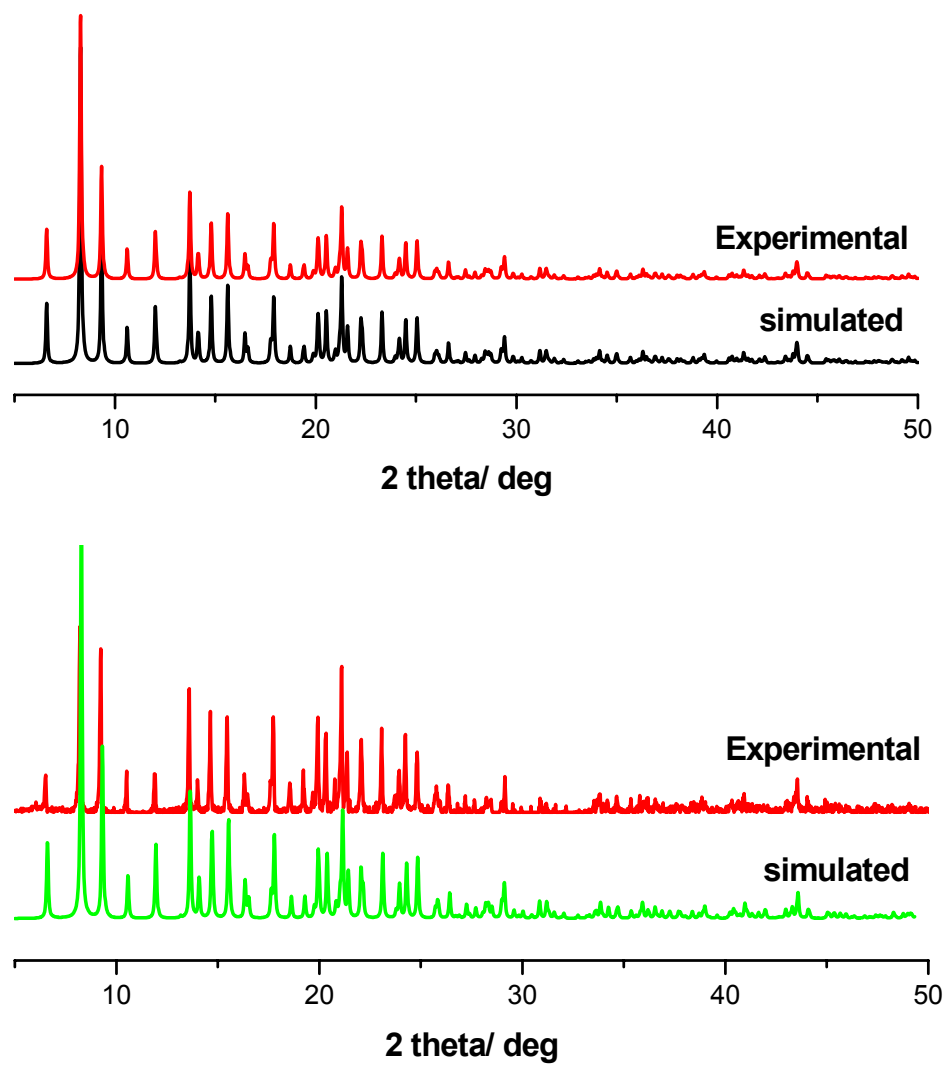


Figure S3. The measured and simulated XRD patterns for Δ -1 (top) and Λ -1 (bottom).